Proceedings of the 2011 International Conference on Advanced Mechatronic Systems, Zhengzhou, China, August 11-13, 2011

SEMG Feature Extraction Methods for Pattern Recognition of Upper Limbs

Feng Zhang, Pengfeng Li, Zeng-Guang Hou, Yixiong Chen, Fei Xu, Jin Hu, Qingling Li, Min Tan

***Abstract*— In this paper, a new feature of surface electromyography (sEMG) by using discrete wavelet transform (DWT) is proposed for motion recognition of upper limbs, and this method can be eventually used for rehabilitation robot control. Seven traditional features of sEMG are also extracted for comparative study, they are integral of absolute value (IAV), difference absolute mean value (DAMV), zero crossing (ZC), variance (VAR), mean power spectral density (MPSD), mean frequency (MF) and median frequency (MDF) respectively. For comparing the recognition rate of the different motions of the upper limb, each feature or their combination are used to construct the feature vectors, and the BP neural network with variable learning rate back propagation with momentum (GDX) algorithm is used to classify these motion modes. The experimental results summarize that the new feature extracted by using DWT presents a higher recognition rate (98.9%) than all of the traditional features, and the traditional features combination can also greatly improve the recognition rate (99%).**

I. INTRODUCTION

There has been more and more people who suffered from spinal cord injury (SCI) or stroke in the world. The treatment to them is a long way because that the neurological damage is very hard to recover. In clinics, the most common method for SCI or stroke rehabilitation is locomotor training, such as treadmill exercise or pedal exercise. Traditional locomotor training machines can just help the patients do passive exercise, and the active movement which has been proven more useful for neurological rehabilitation [1], [2], [3] can not be motivated. We have designed a rehabilitation robot for lower limbs [4], passive exercise or active exercise can been implemented based on this platform.

For arousing the interests of patients in rehabilitation training, surface electromyography (sEMG) can be used to detect the movement intent. SEMG is a weak electrical potential which is generated by the muscle cells [5] when these cells are electrically or neurologically activated, and it is detected from superficial muscles by using surface electrodes. The sEMG has many applications, for example, doctors in hospital use sEMG for the diagnosis of neurological and neuromuscular problems, biomedical engineers or rehabilitation professionals use sEMG as a control signal for prosthetic devices such as prosthetic hands, arms, and lower limbs [6], [7], [8].

Traditionally, sEMG signals are often used as a control signal in three ways. The first method is studying the relationship between sEMG and muscle force [9], [10], [11], [12], the second method is studying the relationship between sEMG and the exact body posture [13], [14], [15], and the third method is studying the pattern recognition of sEMG for different motion modes [16], [17], [18]. Specifically, for the first aspect of sEMG application, peoples are committed to find the relationship between sEMG and muscle forces, thus many muscle force models has been built, such as Hill muscle model [19] and Hammerstein muscle model [20]. Once the exact relationship be found, the patients' active force or torque which also present the patients' movement intention can be detected by the sEMG signals, and active training of the rehabilitation robot are often controlled in this manner. For example, in article [9], Christian provided two approaches for active training of the exoskeleton robots by using sEMG, one is dynamic human body model (DHBM), and the other is direct force control (DFC), and the sEMG is mainly used to compute the force the human body exerts onto the robots. For the second aspect, peoples are committed to find the relationship between sEMG and the exact body posture. This question can also be described as calculating the angle joint of body limbs according to sEMG. Once the exact mapping relationship be found, the exoskeleton robots or prosthetic devices can be controlled to arbitrary feasible posture which is very meaningful for rehabilitation training. For example, in article [13], Artemiadis provide a switching regime model for decoding the sEMG activity of 11 muscles to a continuous representation of arm motion in the 3-D space, by using this method, the position of the arm can been computed just through the sEMG signals. For the third aspect, people are committed to classify different motion modes of human body limbs according to sEMG. High recognition rate and many number of motion modes are two goals for this aspect. Features extraction and classification methods are two key issues. For example, in article [16], the natural logarithm of root mean square values is extracted as the sEMG feature, and a fuzzy C-means clustering method is used for classification of four movements, the recognition rate reached to $92.7\% \pm 3.2\%$. Also in article [21], the author proposed a log-linearized Gaussian mixture network to discriminate sEMG patterns for controlling the human-assisting

This research is supported in part by the National Natural Science Foundation of China (Grant #60775043), the National Hi-Tech R & D Program (863) of China (Grant #2009AA04Z201), and the Sci. & Tech. for the Disabled Program of the Chinese Academy of Sciences (Grant #KGCX2-YW-618)

Feng Zhang, Pengfeng Li, Zeng-Guang Hou, Yixiong Chen, Jin Hu, Qingling Li, Min Tan are with the Laboratory of Complex Systems and Intelligence Science, Institute of Automation, the Chinese Academy of Sciences, Beijing 100190, China feng.zhang@ia.ac.cn

Fei Xu is with the Department of Chemical and Environmental Engineering, China University of Mining and Technology, Beijing, 100083, China xufeicumtb@163.com

manipulator, and this method present high recognition rate (more than 95%) for eight different hand gestures. Yi-Hung Liu proposed a novel sEMG classifier called cascaded kernel learning machine (CLKM) for the motion recognition of upper limbs in [17] and the recognition rate reached to 93.24%.

For patients who have been severely damaged of the lower limbs, sEMG signals can not be detected from lower extremities muscles. Specifically in our research, we try to find a method for rehabilitation robot control by detecting the sEMG signals from the upper limbs. Patients can be trained to produce desirable sEMG characteristics to control the movement of the rehabilitation robot. Through this way, the initiative of the patients can be aroused, and thus can do a better favor to the rehabilitation. The recognition rate is always the most important problem and absolute accuracy is the goal for clinical application. For improving the recognition rate of the upper limbs, a new feature by discrete wavelet transform (DWT) is extracted. For comparison, seven traditional sEMG features including integral of absolute value (IAV), difference absolute mean value (DAMV), zero crossing (ZC), variance (VAR), mean power spectral density (MPSD), mean frequency (MF) and median frequency (MDF) are also extracted. The BP neural network with variable learning rate back propagation with momentum (GDX) algorithm is used for classification. Experimental results summarize that the new feature extracted after DWT present a better a result than the other seven traditional features, and the recognition rate reach to 98.9%. The traditional features combination can also greatly improve the recognition rate (99%).

II. Method

A. Features extraction

There is no doubt that many noise signals will contaminate the original sEMG signals during signals acquisition. The noise signals may come from inherent noise in electronics equipment such as industrial frequency interference (the industrial frequency is 50 Hz in China), DC bias, and baseline noise [22]. Motion artifact which is mainly caused by electrode interface and electrode cable will also cause irregularities in sEMG data [23]. The sEMG signals are also affected by the firing rate of the motor units, and the firing frequency region is 0 to 20 Hz. This kind of noise is considered as unwanted and the removal of the noise is very important [24]. The power density spectra of the sEMG contains most of its power in the frequency range of 5-500 Hz at the extremes [25], [26], so the signals over the high cut-off frequency 500 Hz should be eliminated. After the above discussion, a notch filter with 50 Hz and a band-pass filter with low cut-off frequency 20 Hz and high cut-off frequency 500 Hz should be applied to the raw sEMG signals to remove the noise signal. After the preprocessing, some mathematical transformation such as fast fourier transformation (FFT), wavelet transformation can be done to the sEMG time series, and then a series of features of sEMG can be obtained. In the following two parts, we will introduce seven traditional feature extraction methods and the new feature extraction method by using discrete wavelet transformation (DWT) respectively.

1) Traditional Feature extraction methods: There are seven traditional feature extraction methods we will talk about here. They are list as bellows.

(a) Integral of Absolute Value (IAV)

This feature represents the absolute mean amplitude of sEMG time series and it is a direct reflection of muscle contraction level. IAV of sEMG is calculated as

$$\text{IAV} = \frac{1}{N}\sum_{i=1}^{N}|x_i|, \tag{1}$$

with x_i the ith sample value of sEMG, N the length of sEMG time series.

(b) Difference Absolute Mean Value (DAMV)

The DAMV feature of sEMG calculates all the difference absolute value between every two adjacent sample points along the whole sEMG segment firstly and then calculates the mean value between them. DAMV summarize the vibration amplitude of sEMG signals. The computation formula is as

$$\text{DAMV} = \frac{1}{N}\sum_{i=1}^{N-1}|x_{i+1} - x_i|. \tag{2}$$

(c) Variance (VAR)

VAR of sEMG uses the power of the sEMG signals as a feature. Generally, the VAR is the mean value of the square of the deviation of that variable in statistics, however, as the DC part has been removed in the preprocessing part, then the expression of VAR changes into the following form

$$\text{VAR} = \frac{1}{N-1}\sum_{i=1}^{N-1}x_i^2. \tag{3}$$

(d) Zero Crossing (ZC),

The ZC is the number that the amplitude of sEMG crosses over the zero-amplitude axis. This feature provides an approximate estimation of frequency domain properties. The ZC is calculated as

$$\text{ZC} = \sum_{i=1}^{N-1} sgn(-x_i x_{i+1}), \tag{4}$$

where

$$sgn(x) = \begin{cases} 1, if x > 0 \\ 0, otherwise \end{cases}$$

The above four features are all computed based on sEMG signals amplitude and they are all analyzed in the time domain. The following three features will be analyzed in the frequency domain. The FFT is done to the sEMG signals firstly and then the power spectrum (PS) is calculated.

(e) Median Frequency (MDF) and Mean Frequency (MF)

In article [28], Stulen had a study of the relationship between conduction velocity of the muscle fibers and the MDF, MF, and the ratio of low-frequency components to high-frequency components of the spectrum, and found that the MDF is the preferred parameter. The MDF is the frequency

at which the power spectrum of the sEMG signals is divided into two regions with equal power. It is described as follows

$$\int_0^{\text{MDF}} P(f)df = \int_{\text{MDF}}^{\infty} P(f)df, \tag{5}$$

with $P(f)$ the power spectrum density of sEMG signals and f the frequency of the signal.

The MF is the average frequency and may be expressed by

$$\text{MF} = \int_0^{\infty} fP(f)df \Big/ \int_0^{\infty} P(f)df \tag{6}$$

(f) Mean Power Spectral Density (MPSD)

The MPSD has no practical meaning and there is few articles studying about it, but it is also a statistical nature of the sEMG signals. In this paper, we describe the MPSD as follows

$$\text{MPSD} = \int_0^{\infty} P(f)df \Big/ \int_0^{\infty} df. \tag{7}$$

2) Discrete Wavelet Transformation (DWT): A new method for feature extraction of sEMG signals.

FFT is a most frequently method for frequency domain analysis. However, FFT is limited to a global frequency analysis, and the changes in time can not be detected. Also, the FFT can only be used to reasonably stationary signals, while the sEMG is non-stationary. Wavelet transformations can resolve this problem. By using wavelet transformation, the raw sEMG signals can be decomposed into time-frequency space, and then a time series is decomposed into different frequency bands without crossing throughout the time axis. Further study can be done on the interested frequency band after wavelet transformation.

The mathematical expression of a discrete wavelet family which consists of members or daughter wavelets, $\psi_{jk}(t)$ is obtained by scaling and time shifting of the mother wavelet $\varphi(t)$, and it is defined as follows.

$$\psi_{jk}(t) = \frac{1}{\sqrt{2^j}} \varphi\left(\frac{t - k2^j}{2^j}\right) \tag{8}$$

where $j \in N$ represent the scale number, $k \in Z$ represent the translation parameter. When j becomes large, the basis function ψ_{jk} becomes a stretched version of the prototype, which focuses on the low-frequency components. When j becomes small, the basis function ψ_{jk} becomes a contracted version of the prototype, which focuses on the high-frequency components. However, the shape of the basis wavelet will always remain unchanged.

Once the input signal $x(t)$ is given, the discrete wavelet transformation (DWT) is defined as follows.

$$< x, \psi_{jk} >= \frac{1}{\sqrt{2^j}} \int x(t) \varphi\left(\frac{t - k2^j}{2^j}\right) dt \tag{9}$$

The DWT applies two filters to the raw signals, a low pass filter $G_0(k)$ and a high pass filter $G_1(k)$ [29]. Each filter is followed by a down-sampler, to make the transform efficient. The output of the low pass filter is also called approximation coefficients which is described as c_{jk}, and the output of the high pass filter is called detail coefficients which is described as d_{jk}. The cut-off frequency F_a of the low pass filter and the high pass filter has a relationship with the scale number, the center frequency of the mother wavelet, and also the sample rate. It can be described as follows.

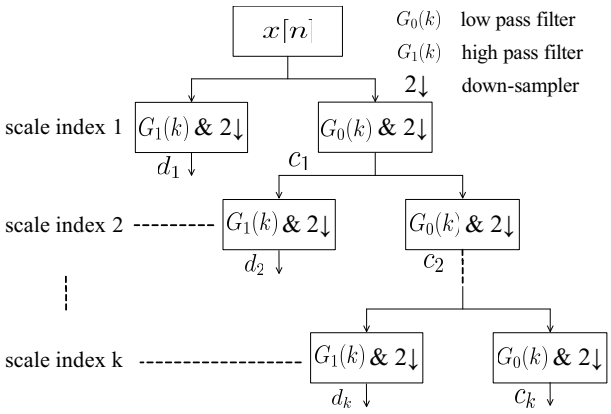

Fig. 1. The DWT decomposition process with the scale number k. The $x[n]$ is the time series of sEMG, and d_1, d_2, d_k are detail coefficients, c_1, c_2, c_k are approximation coefficients.

$$F_a = \frac{F_c \triangle}{2^j} \tag{10}$$

where a is the scale number, $\triangle$ is the sample rate of the raw signals, F_c is the center frequency of the mother wavelet in HZ [30].

For a discrete wavelet transformation (DWT) with the scale index k to a time series of sEMG $x[n]$, the decomposition process is clearly showed in Fig. 1.

B. BP neural network for classification

Once the features of sEMG has been selected for recognition of different types of motions,the next step is choosing a classifier. In this paper, the BP neural network which is very popular for its back propagation algorithm for adjusting the net weights and thresholds is used for pattern classification.

Before using any neural networks, one of the most important things is training the weights and thresholds of the network firstly. Training a neural network needs enough proper sample data, so a large quantity of different sEMG sample data of different muscles for different types of motions should be sampled in a scientific way firstly. There are many back propagation algorithms for training the BP neural network. The steepest descent back propagation is a most basic back propagation algorithm, and the greatest weakness for it is that the learning rate is held constant throughout network training, so the actual performance of the algorithm is very sensitive to the proper selection of the learning rate. Once the learning rate is not properly selected, two problems may be caused. One problem is that the training process may oscillate and become unstable when the learning rate is too big, the other is that the training process is very slow and long time needed for the network convergence [31]. In fact, there is no fixed optimal learning rate for a certain network for the reason that the optimal learning rate changes with

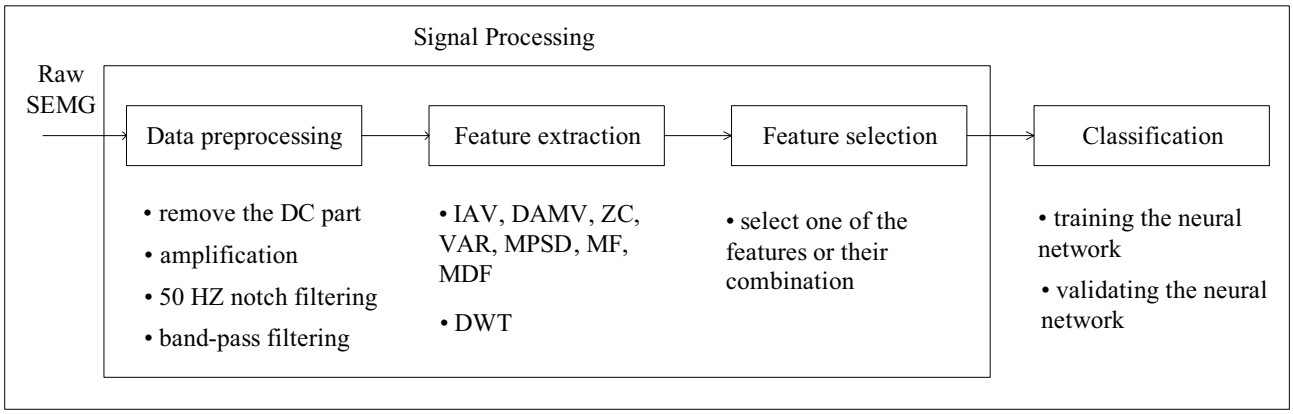

Fig. 2. The flowchart of classifying different types of motions by using sEMG signals.

the iteration number. For the shortage of the steepest descent back propagation, some improved algorithms had been put forward. The variable learning rate BP with momentum (GDX) is one of the improved BP algorithm which is also the algorithm we use in our research.

The variable learning rate BP with momentum algorithm (GDX) can be described as follows.

$$\begin{cases} \triangle x(k+1) = \eta \triangle x(k) + \alpha(k+1)(1-\eta)\dfrac{\partial E(k)}{\partial x(k)} \\ x(k+1) = x(k) + \triangle x(k+1) \end{cases} \quad (11)$$

with

$$\alpha(k+1) = \begin{cases} k_{inc}\alpha(k), E(k+1) < E(k) \\ k_{dec}\alpha(k), E(k+1) > E(k) \end{cases} \quad (12)$$

In eq. (11) and eq. (12), $x(k)$ represents the connection weight vector and the threshold vector between layers for the kth training, $E(k)$ represents the error function which is also the mean square deviation between the desired output and the actual output of the network after the kth training, η is a momentum factor which satisfies $0 < \eta < 1$, $\alpha(k)$ is the learning rate for the kth training, k_{inc} ($k_{inc} > 1$) and k_{dec} ($k_{dec} < 1$) are the incremental factor and decremental factor of learning rate respectively.

From eq. (11) and eq. (12), we can see that the variable learning rate BP with momentum algorithm (GDX) raise the convergence speed from two points of view. Firstly, for the adding of momentum factor η, if the last amendment of the weight and the threshold is too big, the sign of the second item of the first formula in eq. (11) will be contrary to the last amendment, thus the current amendment will be decreased. On the other hand, if the last amendment of the weight and the threshold is too small, the sign of the second item of the first formula in eq. (11) will be same to the last amendment, thus the current amendment will be increased. Clearly it can be seen that the momentum factor always try to increase the amendment along the direction of the same gradient. Secondly, the variable learning rate $\alpha(k)$ always try to make the step length as big as possible on condition that the algorithm is stable. If the error function decreases with the iteration number, it just means that the direction of the adjustment is right and the step length can be increased. On the contrary, if the error function increases with the iteration number, it just means that the direction of the adjustment is wrong and the step length should be decreased.

After above talking, the whole process of classifying different types of motions by using sEMG can be clearly showed in Fig. 2.

III. Experiment and Results

To validate the effectiveness of the features for motion classification of the upper limbs, we implement an experiment on an able-bodied man (26 years old). Four muscles of upper extremity including flexor carpi radialis muscle, extensor carpi ulnaris muscle, extensor pollicis brevis muscle, and flexor digitorum superficialis muscle are selected respectively. Four pairs of Ag/Agcl electrodes with glue solution which can easily stick to the muscle are used for the sEMG signals detection, and each of the electrodes in a pair are separated from each other by 2 cm. The subject is asked to do fist (F), fist unfold (FU), wrist flexion (WF), wrist extension (WE), palm abduction (PA), and palm adduction (PR) respectively, these motions are clearly showed in Fig. 3.

The sEMG signals acquisition equipment we use is FlexComp which is a production of Thought Technology Ltd., Canada. The device can simultaneously capture 10 channels of sEMG data with the sampling rate of 2048HZ for each channel. Before signals acquisition, some small detail works should be done to the selected four muscles, such as shaving and cleaning of the skin surface, these work are mainly to reduce the input resistance and the external disturbance.

Each arm motions can be divided into three steps: rest, action and motion holding. The sEMG signals we extract are during the third step and the signals during this time slice are relatively stable. The data length sustained for 1 second, so there are 2048 sample points of each channel for each motion. After the preprocessing of sEMG that has been talked before, the traditional features including integral of absolute value (IAV), difference absolute mean value (DAMV), zero crossing (ZC), variance (VAR), mean

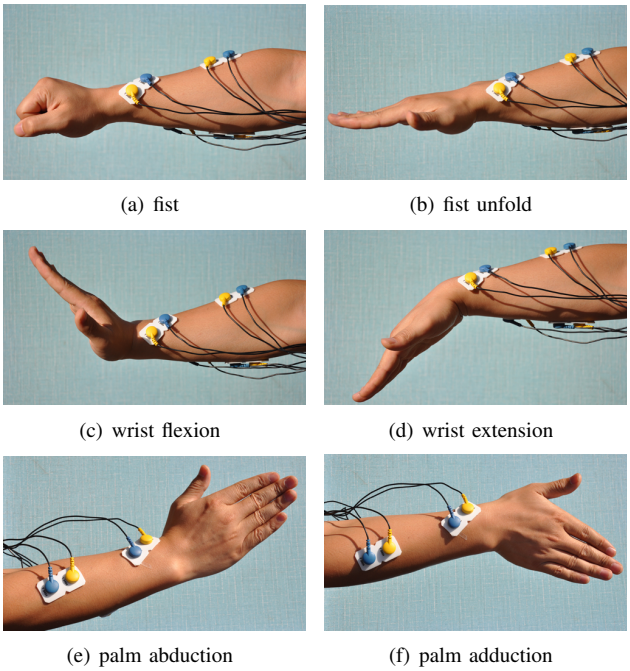

(a) fist (b) fist unfold

(c) wrist flexion (d) wrist extension

(e) palm abduction (f) palm adduction

Fig. 3. Six motions of the upper limb of the right arm

power spectral density (MPSD), mean frequency (MF) and median frequency (MDF) are extracted for each channel respectively. During the computing of the power spectrum for each channel, every 1024 sample points or 0.5s interval with an overlap of 50% is computed respectively, and the average of the power spectrum is calculated. This method is just to reduce the variance in the spectrum estimates and create the characteristic values of the power distribution [30]. For the new method of feature extraction by using discrete wavelet transform (DWT), the mother wavelet we use is Daubechies 05 (db05) and the center frequency of which is 0.6667 HZ. According to the FFT of each channel, we know that the the main power of the sEMG concentrate between 5 HZ and 170 HZ, so we have an idea to extract the information between this frequency band. Also according to equation (10), we know that DWT (db05) with scale number 3 is enough to extract all the information between this frequency band and the integral of absolute value of approximation coefficients were used as the new feature.

For training and validating the BP neural network, each of the six motions were asked to do for 50 times with a five minutes rest between every 10 groups, so there are 300 samples totally, and 210 are used for network training, and 90 are used for network validating. Also for testing the robustness of the BP neural network, there is no limit to the strength when the people do these motions. The BP neural network we use has three layers: input layer, mid layer and the output layer. The number of neurons of the input layer depends on the features used, for example, when only one feature is used for motion recognition, such as IAV, DAMV, ZC, VAR, MPSD, MF, or MDF, then there are four neurons in the input layer, when two features together are used for recognition, then there are eight neurons in the input layer,

TABLE I

RECOGNITION CODE FOR SIX MOTIONS OF UPPER LIMBS

Motion	Code	Motion	Code
fist	100000	fist unfold	010000
wrist flexion	001000	wrist extension	000100
palm abduction	000010	palm adduction	000001

TABLE II

RECOGNITION RATE FOR DIFFERENT FEATURES OR DIFFERENT FEATURE COMBINATIONS

Feature	Recognition rate %	Training error
IAV	92.2	0.0288
DAMV	88.9	0.0315
VAR	91.1	0.0411
MPSD	86.7	0.0562
ZC	47.8	0.157
MDF	77.7	0.0849
MF	72.2	0.0782
IAV+VPR	98.9	0.0167
IAV+MPSD	98.9	0.0245
IAV+DAMV	98.9	0.0306
VAR+DAMV	95.6	0.0390
VAR+MPSD	94.4	0.0407
MPS+DAMV	94.4	0.0218
IAV+DAMV+VAR	99	0.00623
IAV+DAMV+MPSD	99	0.00413
IAV+VAR+MPSD	99	0.00523
DAMV+VAR+MPSD	99	0.00794
DWT	98.9	0.0151

and 12 neurons in the input layer for three features together. The number of neurons in the mid layer is 12 when the number of neurons in the input layer is less than 12, and 20 when the number of neurons in the input layer is 12. The number of neurons in the output layer is always 6, and the output value of each neuron is between 0 and 1. The six motions of the upper limb is represented by six binary codes. The specific representation is showed in Table I. The recognition rate and the training error of the BP neural network are clearly showed in table II.

From table II, we can see that the features ZC, MDF, and MF present a big training error for the BP neural network, and the right recognition rate is relatively small, while the other four features such as IAV, DAMV, VAR, and MPSD present a small training error, and the right recognition rate is more than 86%. Different features combination between IAV, DAMV, VAR, and MPSD can greatly improve the recognition rate, for example, the combination of VAR and MPSD can give a recognition rate of 94.4% and the combination of IAV and VPR can give a recognition rate of 98.8%. Three of the features IAV, DAMV, VAR, and MPSD together can give a recognition rate of 99%. The new feature of sEMG which is computed by DWT also give a high recognition rate of 98.8% which is bigger than that of all the traditional features described above.

IV. CONCLUSIONS

In this paper, a new feature of sEMG signals is extracted by using DWT, and this feature present a good result for

pattern recognition of upper limbs. Although the traditional features such as IAV, DAMV, ZC, VAR, MPSD, MF, and MDF present a bad result, their combination also greatly improved the recognition rate. The BP neural network with GDX algorithm used in this paper also prove that the BP neural network is a good classifier. Many other factors may also affect the recognition rate such as muscles selection and electrodes position. In our future work, we will apply this method to real-time rehabilitation robot control.

REFERENCES

[1] M. Lotze, C. Braun, N. Birbaumer, S. Anders, L.G. Cohen, Motor learning elcited by voluntary. *Brain*, vol. 126, 2003, pp. 866–872.

[2] L.L. Cai, A.J. Fong, C.K. Otoshi, Y. Liang, J.W. Burdick, R.R. Roy, V.R. Edgerton, Implications of assist-as-needed robotic step training after a complete spinal cord injury on intrinsic strategies of motor learning. *Neurscience*, vol. 26, no. 4, 2006, pp. 10564-8.

[3] G. Rosati, P. Gallina, S. Masiero, Design implementation and clinical tests of a wire-based robot for neurorehabilitation. *IEEE Trans. on Neural Systems and Rehabilitation Engineering*, vol. 15, no. 4, 2007, pp. 560–569.

[4] F. Zhang, P.F. Li, Z.G. Hou, X.L. Xie, Y.X. Chen, Q.L. Li, M. Tan, "An Adaptive RBF Neural Network Control Strategy for Lower Limb Rehabilitation Robot", *ICIRA2010*, 2010, 417–427.

[5] G. kamen and D. Gabriel, *Essentials of Electromyography*. USA: Human Kinetics Publishers, 2009.

[6] C. Cipriani, F. Zaccone, S. micera, M.C. Carrozza, On the shared control of an EMG-controlled prosthetic hand: analysis of user-prosthesis interaction, *IEEE Trans. on Robotics*, vol. 24 no. 1, 2008, pp. 170–184.

[7] T.A. Kuiken, G. Li, B.A. Lock, R.D. Lipschutz, L.A. Miller, K.A. Stubblefield, K.B. Englehart, Targeted muscle reinnervation for real-time myoelectric control of multifunction artificial arms, *Journal of American Medical Association*, vol. 301, no. 6, 2009, pp. 619–628.

[8] Y. Oonishi, O. Sehoon, Y. Hori, A new control method for power-assisted wheelchair based on the surface myoelectric signal, *IEEE Trans. on Industrial Electronics*, vol. 57 no. 9, 2010, pp. 3191–6.

[9] C. Fleischer, A. Wege, K. Kondak, and G. Hommel, Application of EMG signals for controlling exoskeleton robots, *Biomed Tech*, vol. 51, 2006, pp. 314–319.

[10] C. A. M. Doorenbosch and J. harlaar, Accuracy of a practicable EMG to force model for knee muscles, *Neuroscience Letters*, vol. 368, 2004, pp. 78–81.

[11] G. L. David and F. B. Thor, An EMG-driven musculoskeletal model to estimate muscle forces and knee joint moments in vivo, *Journal of Biomechanics*, vol. 36, 2003, pp. 765–776.

[12] Q. Shao, N. B. Daniel, K. Manal, and S. B. Thomas, An EMG-driven model to estimate muscle forces and joint moments in stroke patients, *Computers in Biology and Medicine*, vol. 39, 2009, pp. 1083–1088.

[13] P. K. Artemiadis and K. J. Kyriakopoulos, A switching regime model for the EMG-based control of a robot arm, *IEEE Trans. on Systems, Man, and Cybernetics-Part B: Cybernetics*, vol. 99, 2010, pp. 1–11.

[14] S. Au, P. Bonato, and H. Herr, "An EMG-position controlled system for an active ankle-foot prosthesis: an initial experimental study", *ICORR 9th International Conference on Rehabilitation Robotics*, 2005, pp. 375–379.

[15] P. K. Artemiadis and K. J. Kyriakopoulos, EMG-based position and force estimates in coupled human-robot systems: towards EMG-controlled exoskeletons, *Springer Tracts in Advanced Robotics*, vol. 54, 2009, pp. 241–250.

[16] K. Momen, S. krishnan, and T. Chau, Real-time classification of forearm electromyographic signals corresponding to user-selected intensional movements for multifunction prosthesis control, *IEEE Trans. on Neural Systems and Rehabilitation Engineering*, vol. 15, 2007, pp. 535–542.

[17] Y. H. Liu, H. P. Huang, and C. H. Weng, Recognition of electromyographic signals using cascaded kernel learning machine, *IEEE Trans. on Mechatronics*, vol. 12, 2007, pp. 253–264.

[18] D. Tkach, H. Huang, and T. Kuiken, Study of stability of time-domain features for electromyographic pattern recognition, *J Neuroeng Rehabil.*, vol. 5, 2010, pp. 7–21.

[19] A. V. Hill, The heat of shortening and the dynamic constants of muscle, *Proceedings of Royal Society London B*, vol. 126, 1938, pp. 136–195.

[20] K. J. Hunt, M. Munih, N. de N. Donaldson, and F. M. D. Barr, Investigation of the hammerstein hypothesis in the modeling of electrically stimulated muscle, *IEEE Trans. on Biomedical Engineering*, vol. 45, no. 8, 1998, pp. 998–1009.

[21] O. Fukuda, T. Tsuji, M, kaneko, A. Otsuka, A human-assisting manipulator teleoperated by EMG signals and arm motions. *IEEE Trans. on Robotics and Automation*, vol. 19, no. 2, 2003, pp. 210–222.

[22] F.L. Laura, K. Chandramouli, A. Keith, Modeling nonlinear errors in surface electromyography due to baseline noise: A new methodology. *Journal of Biomechanics*, vol. 44, 2011, pp. 202–5.

[23] C.J. De Luca, L.D. Gilmore, M. Kuznetsov, S.H. Roy, Filtering the surface EMG signal: Movement artifact and baseline noise contamination. *Journal of Biomechinics*, vol. 43, no. 8, 2010, pp. 1573–9.

[24] M.B.I. Raez, M.S. Hussain, F. Mohd-Yasin, Techniques of EMG signal analysis: detection, processing, classification and applications. *Biol Proced Online*, vol. 8, 2006, pp. 11–35.

[25] A. van Boxtel, Optimal signal bandwidth for the recording of surface EMG activity of facial, jaw, oral, and neck muscles, *Psychophysiology*, vol. 38, no. 1, 2001, pp. 22-34.

[26] A. van Boxtel, A.J. Boelhouwer, A.R. Bos, Optimal EMG signal bandwidth and interelectrode distance for the recording of acoustic, electrocutaneous, and photic blink reflexes, *Psychophysiology*, vol. 35, no. 6, 1998, pp. 690-7.

[27] C. J. D. Luca, *Surface Electromyography: Detection and Recording*. Boston, MA: Delsys Incorporated, 2002.

[28] F. B. Stulen, D. Luca, and J. Carlo, Frequency parameters of the myoelectric signal as a measure of muscle conduction velocity, *IEEE Trans. on Biomedical Engineering*, vol. 28, 1981, pp. 515–523.

[29] H. S. M. Reddy and K. B. Raja, High capacity and security steganography using discrete wavelet transform, *International Journal of Computer Science and Security*, vol. 3, 2009, pp. 462–472.

[30] J. Kilby, G. Mawston, and H. Gholam, Analysis of surface EMG singnals using continuous wavelet transform for feature extraction, *Advances in Medical, Signal and Information Processing*, 2006, pp. 1–4.

[31] V. N. P. Dao and R. Vemuri, A performance comparison of different back propagation neural networks methods in computer network intrusion detection, *Differential Equations and Dynamical Systems*, vol. 10, 2002.